Hexacopter Flight Dynamics on Earth and Martian Surfaces

Raghuvir Singh
Aerospace Engineer
NASA Ames Research Center
Moffett Field, CA, USA

ABSTRACT

Since the atmospheric conditions and gravitational field are different for Mars and Earth, the operating flight environments are different, and necessitate Earth-based appropriate modeling, analysis, and simulation for Mars flight vehicles. This paper compares a hexacopter's flight dynamics in the two environments. The analysis is necessary to determine if a dynamically matched surrogate hexacopter can be designed to conduct reliable testing on Earth, with the goal of successfully operation on Mars. To answer the question, the comprehensive tool FLIGHTLAB® is used to model the hexacopter flight dynamics. Frequency responses in heave, pitch, roll, and yaw rates of the hexacopter in hover are analyzed. The simulation result shows that each attitude response of the designed hexacopter responds very differently in the two environments. The closed-loop response of the hexacopter can be made stable on Earth but not on Mars. Therefore, the proportional feedback technique cannot be utilized to stabilize all four responses altogether. Due to the dynamics of the model being very different in each atmosphere, it is yet not feasible to create a dynamically matched surrogate helicopter that can operate in both environments.

INTRODUCTION

Mars, known as the Red Planet, provides an ideal terrestrial laboratory to understand the early history of the solar system. The planets Mars, Venus, and Earth all formed from the same minerals and elements; however, all three planets went through different epochal periods. Mars's surface pressure is 1% of the surface pressure of the Earth (Ref. 1). Moreover, Mars has a history of dehydration and, loss of its atmosphere, and surface. Research is being conducted to understand Mars transformation as a planet. Specifically, NASA's Mars Exploration Program is studying the formation and early evolution of Mars as a planet, the history of geological processes, the potential for Mars to have hosted life, and the future exploration of Mars by humans.

Orbiters like MAVEN (2003) helped explore the upper atmosphere of Mars whereas, stationary landers like Insight (2018) made it possible to detect quakes on Mars and revealed details about the depth and composition of Mars's crust, mantle, and core (Ref. 2). Furthermore, the Perseverance rover helped understand the dust processes on Mars and contributed to a body of knowledge that could one day help predict the dust storms that Mars is famous for, which poses a threat to future robotic, and human explorers. Rovers are also designed to seek evidence of life, study rocks and soil in situ and collect soil samples to return to Earth (Ref. 1). Even though stationary landers and rovers have transverse great distances in search of new scientific information, the aerial dimension of Mars exploration is still yet to be fully exploited (Ref. 3). Ingenuity (2021), a technology demonstrator, paved the way for future aerial explorers at Mars which is discussed later in the paper.

Flying on Mars constitutes a set of challenges and requirements. The challenges are imposed due to the Martian atmosphere being very different when compared to Earth's atmosphere. Carbon dioxide composes 95.32% of the Martian atmosphere while the remaining 4.68% is composed of argon, oxygen, carbon monoxide, water vapor, and trace gasses (Ref. 4). Moreover, Mars experiences a temperature range from -140 C at the poles to up to 30 C on the equator during daytime (Ref. 5). Besides the high variance in temperature, Mars's atmosphere is also very different from Earth's in numerous other ways. The pressure on Mars averages 6.36 millibars which is 0.6% of the Earth's atmospheric pressure (Ref. 4). Air density at the Mars surface is about 0.02 kg/m^2. Furthermore, Mars's gravitational acceleration is about one-third of Earth's gravitational acceleration (Ref. 4). Lower gravitational pull should result in greater lift capability, yet the reduction in lift due to different atmospheric conditions eliminates this advantage.

The challenges of flying on Mars put greater reliance on using simulation tools that can replicate Martian flight environments. This paper provides a flight dynamics

Presented at the VFS 6th Decennial Aeromechanics Specialists' Conference, Santa Clara, CA, USA Feb.6-8, 2024. This is a work of the U.S. Government and is not subject to copyright protection.

comparison of a hexacopter in a hover state using a state of the art comprehensive analysis tool - FLIGHTLAB. The comparison of flight dynamics in the two different environments helps determine if a dynamically matched surrogate helicopter can be designed, such that the resulting model can be used to conduct flight testing on Earth during the aircraft development cycle on Earth.

BACKGROUND

The idea of flying on Mars has been around since the early days of space exploration. The idea of flying in a thin, cold, and CO_2 based environment became prevalent after the Viking Lander Mission of the 1970s (Ref. 2). The idea of flying on Mars using compressed gas was first introduced by Savu and Trifu in the mid-1990s (Ref. 6). Soon after, the Stanford University tested a small rotorcraft under Mars's atmospheric conditions in the Jet Propulsion Laboratory (JPL) vacuum chamber (Ref. 7). Even though no data was published from the above research, they certainly opened the arena of the possibility of flying on Mars. NASA Ames conducted research on rotorcraft conceptual designs for Mars exploration. Young, Chen, and Briggs discussed the challenges associated with developing autonomous vertical-lift planetary aerial vehicles (Ref. 8) and concluded that vertical-lift planetary aerial vehicles could potentially be developed for planets like Mars and Venus. Following the research, the University of Maryland (Ref. 9) and Georgia Institute of Technology (Ref. 10) developed potential designs for Martian rotorcraft. The University of Maryland produced the Martian Autonomous Rotary Wing Vehicle (MARV). MARV was a coaxial helicopter designed to carry a payload of 10.8 kg with an endurance of 39 min. Separately, the Georgia Institute of Technology developed a quad-rotor design (GTMARS) with rotors of 1.84 m in diameter and endurance of 30 min. Figure 1 shows the MARV design and Figure 2 shows the GTMARS design.

Figure 1. MARV (Ref. 9)

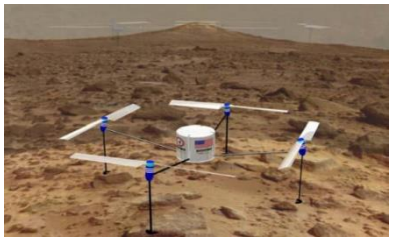

Figure 2.GTMARS (Ref. 10)

Georgia Institute of Technology also produced the Mars UAV concept. Figure 3 illustrates the concept, a combination of a ground rover and a rotary-wing UAV, designed to be used for exploration purposes. Tohoku University (Ref. 11) also developed a four-rotor conceptual design (JMH) shown in Figure 4.

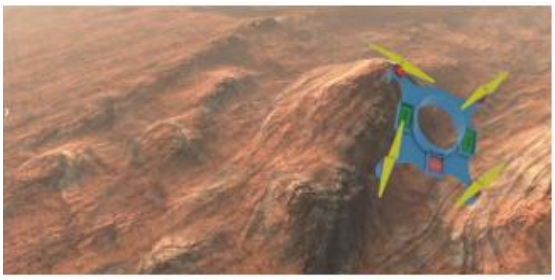

Figure 3. Mars UAV (Ref. 10)

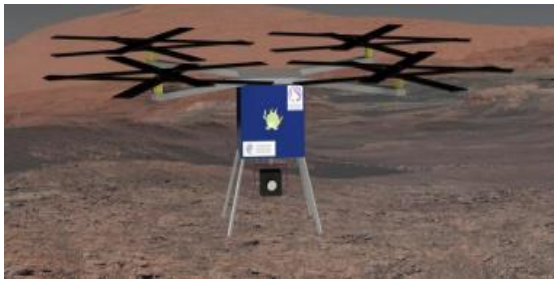

Figure 4. Japanese Mars Helicopter (JMH) (Ref. 11)

Following the developments described above, the technology demonstrator Ingenuity was developed as a collaboration between the JPL, NASA Ames Research Center, and NASA Langley Research Center (Ref. 12). Ingenuity features a coaxial rotor system with counter-rotating hingeless two-bladed rotors. The vehicle is controlled using both upper and lower swashplates which provide both collective and cyclic control.

Differential collective is used to achieve yaw control while keeping the rotor speed constant. Figure 5 shows a CAD model and Table 1 shows Ingenuity vehicle characteristics.

Figure 5. Mars Helicopter Ingenuity (Ref. 12)

Table 1. Ingenuity specifications

Parameter	Value
Total Mass	1.8 kg
Rotor Diameter	1.21 m
Rotor Spacing	0.1 m
Ground Clearance (lower Rotor)	0.3 m
Landing gear footprint	0.6 X 0.6 m
Thrust-Weight ratio	135 to 155%
Endurance	$\geq$ 1.5min
Rotor Speed	$\leq$ 2800 rpm
Collective control (both rotors)	-4.5 to 17.5 deg
Cyclic control (both rotors)	$\pm$10 deg

Challenges of Flying on Mars

As mentioned before, flying on Mars involves a set of challenges and requirements. The challenges are imposed due to the Martian atmosphere having large daily temperature ranges, and lower density. The difference in atmosphere highly influences both the fight dynamics and design of a vehicle. Mars's atmosphere also presents some challenges in testing, verification, and validation of a model as it is difficult to fully replicate the Martian atmosphere on Earth. This results in a heavy reliance on modeling and analysis tools that can run simulations in user-defined environments.

Flap Dynamics on Mars

Compared to the flight dynamics of stationary airfoils relative to their body frame (i.e., fixed-wing aircraft), helicopter flight dynamics are much more complicated due to having rotating airfoils relative to the body frame and the influence of the wake-induced inflow distribution on rotors. Periodic forces and moments are produced by the asymmetry produced by forward flight, control inputs and/or environmental disturbances. Blade flap damping is affected by the density difference between Earth and Mars

To understand blade flapping on Mars, a simpler model of a rod rotating about a hinge is considered. Figure 6 shows an illustration of the blade model being considered.

Figure 6. Blade flapping modeled by a central hinge (Ref. 12)

The model shown in Figure 6 acts as a classical mass-spring-damper system. Centrifugal force and structural stiffening create a restoring moment on the hinge. Damping is present due to the aerodynamic forces. When cyclic pitch is applied to a helicopter blade, a periodic change in lift is produced at the rotor frequency, with maximum lift on one side of the rotor disk, and minimum lift on the opposite side. Given the above conditions, a blade responds like a mass spring damper, flapping with the same frequency, but with a different phase than the input (Ref. 12). Aircraft roll and pitch moments are generated through a combination of the tilting of the thrust vector due to blade flapping and direct hub moments due to resistance against flapping at the hub. (Ref 13). Figure 7 shows the magnitude and phase response of a centrally hinged blade flap angle response to 1-degree blade pitch input in both Earth's and Mars's density. The blue line represents the response to the input pitch cyclic in Earth's atmosphere. The green line represents the response in Mars's atmosphere. The red line represents the rotor frequency. In the Earth's atmosphere, the peak flap output occurs 90 ° after the peak cyclic pitch input due to rotor speed coinciding with the natural frequency of the mass-spring-damper. Specifically, a peaking cyclic input applied on the right-hand side of the vehicle will result in a nose-up moment. Change in response is noticed due to reduced aerodynamic damping with a decrease in density (damping reduced to 2% in Figure 7). In Mars's atmosphere, the phase angle drops to near zero around the natural frequency if the rotor is stiffened to increase the natural frequency.

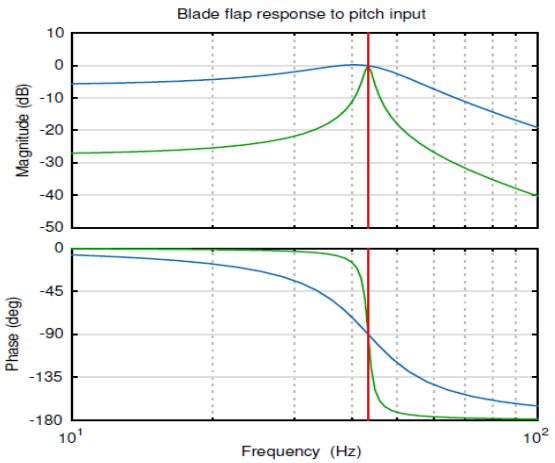

Figure 7. Magnitude and phase response of a blade flap response to pitch input for a centrally hinged blade with no additional stiffness; blue Earth, green Mars (Ref. 12)

HEXACOPTER OVERVIEW

The vehicle presented in this paper is a rotorcraft with six rotors, commonly known as a hexacopter. The hexacopter is designed to fulfill a Mars science flight mission (Figure 8). The hexacopter should be able to take off in 30 seconds and climb 200m above its landing site. It must have a cruising range of 1km along with the capability to hover over the science site for 2 min. Lastly, it should be able to land and recharge (Ref. 13).

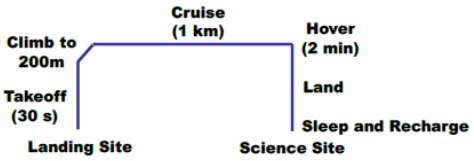

Figure 8. Hexacopter flight mission (Ref. 13)

The design of the hexacopter is constrained by the size of the aeroshell that will be used to transport the vehicle from Earth to Mars. A spreadsheet was designed by NASA Ames Research Center that sized and produced initial estimates. The estimates considered sizing constraints imposed by the size of an aeroshell in which the vehicle needs to be folded and packaged before being transported to Mars's surface (Ref. 13).

The hexacopter weighs 17.8 kg and features six four-bladed rotors. All six rotors are hingeless and are 0.64 m in radius. The rotors operate at 2782 RPM in Mars's atmosphere and 600 RPM in Earth's atmosphere. The difference in RPM between each atmosphere is to achieve the same blade lift coefficient in both atmospheres.

(1) $$\frac{C_T}{\sigma} = \frac{T}{\rho A_b (\omega R)^2}$$

In eq. (1) T is the rotor thrust, A_b is the total blade area, ω is the rotor rotational speed, ρ is the density, and R is the rotor radius. Rotors rotational speed is increased in Mars's atmosphere to compensate for the reduce in density compared to that on Earth. All rotors are controlled via collective pitch control that changes the amount of thrust produced by rotors. Differential collective produces a yaw moment, whereas a combination of change in the thrust of specific rotors produces both roll and pitch moments. The vehicle is designed to carry a payload of 2.02 kg and has a range of 2 km. The vehicle is also able to cruise at 30 m/s (ref. 13).

Figure 9. Hexacopter model (Ref. 13)

FLIGHTLAB MODELING

To understand the flight dynamics of the hexacopter, FLIGHTLAB, a finite element, multi-body, selective fidelity modeling, and analysis software package is used to simulate the hexacopter in both Earth and Mars environments. FLIGHTLAB allows users to build a model using structural, aerodynamic, control, and solution components. Once a model is built in the FLIGHTLAB environment, the model (vehicle) can be simulated in any user-desired atmosphere.

The hexacopter model consists of a fuselage, the mast, and the rotor blades. The fuselage of the hexacopter is modeled as a rigid fuselage with six non-linear degrees of freedom with inertial and mass properties. The mast of the hexacopter is modeled as a point mass with no inertial or mass properties. The rotor blades are modeled as rigid blades with flapping dynamics. The aircraft is controlled via collective pitch.

Aerodynamic Forces and Moments

The aerodynamic forces and moments on rotor blades can be determined by splitting the rotor blade into multiple sections with individual span, chord, twist, and sweep. For the hexacopter each blade is divided into five sections. Each section of the blade is associated with lift, drag, and moment coefficient as a function of angle of attack and Mach number. Blade Element Theory is used to calculate the entire performance of each of the six rotors. The theory is based on the lifting-line assumption and neglects any stall and compressibility effects on rotor performance. Based on the theory, eq (2) describes the air velocity seen by the blade, where, U_T, U_P are the tangential, and normal air velocity component respectively.

(2) $$U = \sqrt{U_T^2 + U_p^2} \cong U_T$$

The two-dimensional quasi-steady aerodynamic theory is used to compute wing/blade segment airloads with respect to angle of attack and Mach number. Lift eq (3) and drag eq (4) are computed in terms of air velocity.

(3) $$L = \frac{\rho}{2} U^2 c\{a(\theta - \phi_a) + c_0\}$$

(4) $$D = \frac{\rho}{2} U^2 c c_{d0}$$

In the above equations, a is the lift slope, c_0 is the lift at zero angle of attack, c is the chord length, θ is the blade pitch angle, ϕ_a is the induced angle which is simplified by a small angle assumption so that the angle $\phi_a \cong \frac{Up}{UT}$, and L and D are lift and drag per unit length.

The drag produced by the fuselage is not a function of the angle of attack as none of the aerodynamic properties of the fuselage are modeled.

Induced Velocity

The model uses a three-state induced inflow model derived from the Peters/He finite state model. The finite state dynamic wake model uses state space formulation and can model the rotor wake dynamics. To obtain a solution, the finite state model enforces boundary conditions such that the pressure function matches the blade loading on the rotor blades and is zero at infinity. The induced flow distribution (w) at the rotor plane is represented at a desired harmonic, N, for each harmonic, a specific number of radial shape function, S_r,.

(5)

$$w_i(\hat{x}, \psi, t) = \sum_{r=0}^{N} \sum_{j=r+1,r+3\ldots}^{2S_r+r-1} \phi_j^r(\hat{x})[\alpha_j^r(t)\cos(r\psi) + \beta_j^r(t)\sin(r\psi)]$$

$\hat{x}$ is the radial coordinate, ψ is the azimuth position, and t is time. The dynamic wake in the tip path plane is modeled as a set of first order ordinary equations which relates the inflow states to the induced inflow forcing functions.

(6) $$M\dot{x} + Lx = \tau$$

Where M is the apparent mass of the system and is computed as,

(7) $$[M] = \begin{bmatrix} [M^c] & 0 \\ 0 & [M^s] \end{bmatrix}$$

The apparent stiffness, L, is computed as,

(8) $$[L] = [T]^T \begin{bmatrix} [L^c]^{-1} & 0 \\ 0 & [L^s]^{-1} \end{bmatrix} [T]$$

The coefficients of the dynamic wake in the tip path plane are described in detail in the FLIGHTLAB theory manual (Ref. 14).

Trim and Linearization

An equilibrium point is required to obtain the desired linear time-invariant model for flight dynamic analysis. Linear time-invariant models allow frequency domain analysis that can be used to understand the flight dynamics of the designed vehicle. FLIGHTLAB is used to obtain an equilibrium point of the vehicle by using the process of Newton-Raphson method. The Newton-Raphson method is an iterative process that finds the root of an equation by linear approximation. In other words, a nonlinear function is approximated by a linear function tangent to it. Figure 10 shows a geometric interpretation of the Newton-Raphson method.

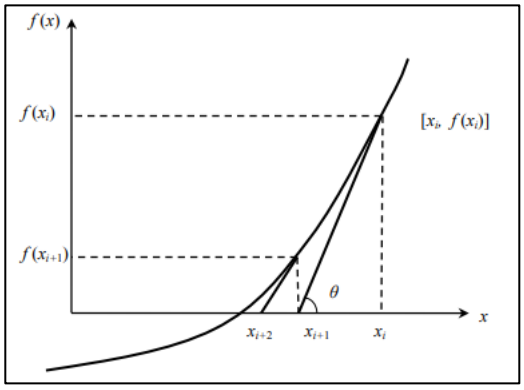

Figure 10. Newton Raphson method illustration

The figure illustrates the principle of linear approximation point. x_i is the initial root guess of nonlinear function $f(x) = 0$. The Newton-Raphson method approximates an improved estimate of the root by fitting a tangent line to the curve at point x_i. The point of intersection where the tangent intersects the x-axis is the improved estimate of the root i.e. x_{i+1}. The process is iterated until the desired root is obtained. For example, a generalized force is set equal to nonlinear equations

(9) $$Q = f(\ddot{x_2}, \dot{x_2}, x_2, \dot{x_1}, x_1, u)$$
$$y = g(\ddot{x_2}, \dot{x_2}, x_2, x_1, \dot{x_1}, u)$$

In eq. (9), Q is the imbalance in satisfying the differential equations. u are the inputs to the component and y represents the outputs from the component. The objective is to find a set of states and their derivatives that drive Q to zero such that Q=0. If the equations are coupled with more than one solution component, then the coupled/assembled equations are used to find the states and derivatives that derive the generalized forces for all components to within an acceptable tolerance close to zero. Each state and derivative are perturbed one by one to calculate the change in all generalized forces. The nonlinear state equations for a multi-component solution group can be written as,

(10) $$\delta Q_1 = C_{11}\delta\dot{x}_1 + K_{11}\delta x_1 + M_{12}\delta\ddot{x}_2 + C_{12}\delta\dot{x}_2 + K_{12}\delta x_2$$

(11) $$\delta Q_2 = M_{22}\delta\ddot{x}_2 + C_{22}\delta\dot{x}_2 + K_{22}\delta x_2 + C_{21}\delta\dot{x}_1 + K_{21}\delta x_1$$

Where, M, C, and K are the mass, damping, and stiffness partials respectively. Newton-Raphson process is carried out to estimate the change in the states and the derivatives that are required to drive the generalized force, Q, to near zero. Due to the equation being nonlinear, an iterative approach is used to obtain the change in Q. Equation (12) shows the current iteration which is assumed to be the negative value of Q at the previous step.

(12) $$\delta Q^i = -Q^{i-1}$$

FLIGHTLAB uses a method to solve the nonlinear state and output equations which computes the value of Q at each time step. The method determines the level of linearization and the nature of discretization. The highest derivatives terms are linearized using the Newton-Raphson method.

(13) $$\delta Q_1^i = C_{11}\delta\dot{x}_1^i + M_{12}\delta\ddot{x}_2^i = -Q_1^{i-1}$$

(14) $$\delta Q_2^i = C_{21}\delta\dot{x}_1^i + M_{22}\delta\ddot{x}_2^i = -Q_2^{i-1}$$

The above equation can be written as,

(15) $$\delta Q^i = M\delta x_{hd} = -Q^{i-1}$$

The highest order derivate x_{hd} is solved and the inverted mass matrix is computed by time discretization.

(16) $$x_{hd}^i = x_{hd}^{i-1} - Minv * Q^{i-1}$$

Equation (16) is the approximate solution. The used method is called repeatedly until a suitable degree of convergence is achieved.

LINEAR MODEL EXTRACTION AND VALIDATION

The linear state space matrices in the form of $\dot{x} = Ax + Bu$ were extracted through FLIGHTLAB to generate frequency Bode plots. Frequency Bode plots are generated to understand the system response by taking raw measurements of the output amplitude and phase of the system undergoing a sinusoidal input. Frequency responses are also helpful in determining the stability of a closed-loop system.

Flight Dynamic Analysis in Earth's Atmosphere

To validate the linear models obtained from FLIGHTLAB, the non-linear dynamics of the hexacopter were also linearized in CAMRAD II (Ref. 15). Both linearized models were input into MATLAB and the bode function was used to compare the flight dynamics of the model. Figure 11 shows the eigenvalue comparison between CAMRAD II and FLIGHTLAB models in Earth's atmosphere. Both sets of eigenvalues align very closely and predict similar damping characteristics of the hexacopter in Earth's atmosphere. The difference is due to the difference in modeling inflow which is explained later in this section. The figure also shows flapping modes at a frequency range of 420 to 600 rad/s, and airframe modes at low frequency from 0.1 to 100 rad/s. Inflow modes also exist at the mid-frequency range of 340 to 420 rad/s.

In Figure 12, FLIGHTLAB shows all poles of the system in the left half plane, predicting a stable system whereas, CAMRAD II shows one set of poles in the right half plane, thus predicting the unstable behavior of the hexacopter in Earth's atmosphere.

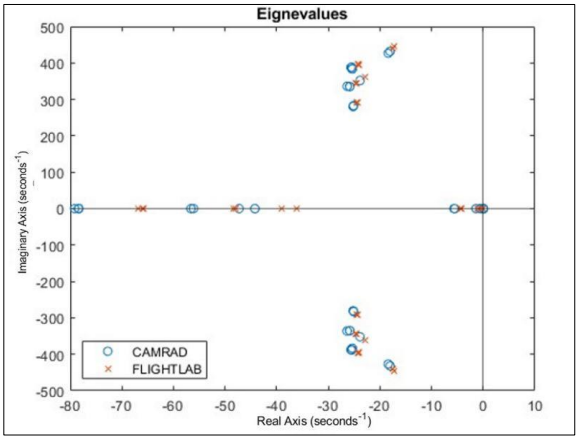

Figure 11. Eigenvalues of the hexacopter in Earth's atmosphere

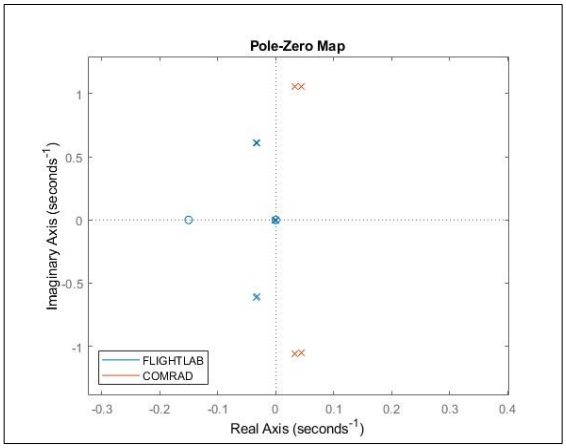

Figure 12. Pole zero map (Earth's atmosphere)

A slight difference in inflow modes is observed between the FIGHTLAB and CAMRAD II linear models (Figure 11). Both tools use momentum potential flow theory to conduct rotor wake analysis. The difference is due to CAMRAD II using a wake distortion factor (κ) of 1.15. No wake distortion factor or states are included in the linearized model obtained from FLIGHTAB. Furthermore, the modes retrieved from the CAMRAD II linear model are slightly more damped than the ones retrieved from FLIGHTLAB.

FLIGHTLAB frequency responses of the hexacopter were also extracted and compared against the CAMRAD II linear

model. Figure 13 and Figure 14 show the heave frequency response to collective input and yaw rate response to pedal input respectively. Both responses are plotted from 0.1 rad/s to 1000 rad/s. For both heave and yaw rate, the results obtained from FLIGHTLAB align very closely with the results obtained from CAMRAD II, thus validating the response produced by FLIGHTLAB. The responses are first order with a rotor mode present at a higher frequency. This is the regressive mode which is generated at the frequency of $\upsilon_{flap} - 1$/rev, where, υ_{flap} is the flap frequency of the coning mode. For both heave and yaw rates, the regressive mode is generated at approximately 371 rad/s. The coning mode is theoretically at the same frequency as the rotating natural flap frequency. Specifically, a coning would be seen at approximately 430 rad/s. Furthermore, the system is also damped which is expected when operating in Earth's atmosphere. This is confirmed by the gradual decrease in the phase angle. For flight control purposes, the FLIGHTLAB heave response shown in Figure 13 is acceptable as no modes are present in the mid-range frequency (rad/s) and the response matches very closely to the one obtained from CAMRAD II.

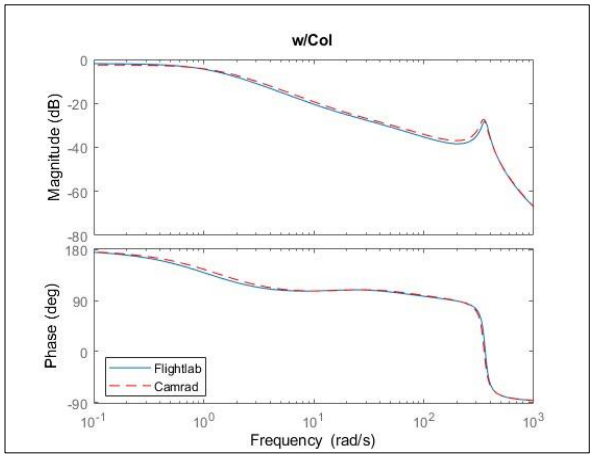

Figure 13. Heave response to collective input

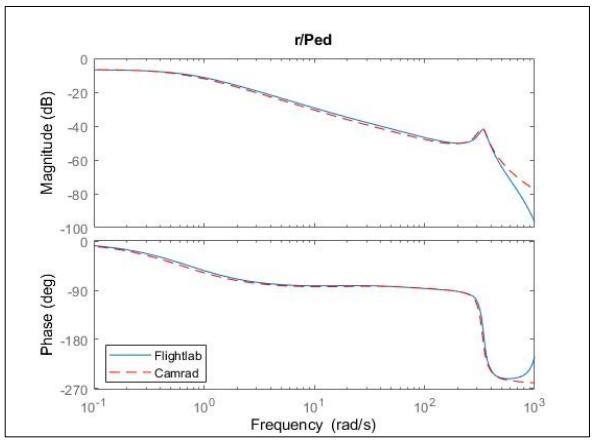

Figure 14. Yaw rate response to pedal input

Figure 15 and Figure 16 shows the pitch and roll rate response of the hexacopter in Earth's atmosphere. Both the characteristics and magnitude of FLIGHTLAB and CAMRAD II linear models align very closely with each other with a difference in frequency for the phugoid mode. The difference is due to FLIGHTLAB linear models missing inflow states and not using the wake distortion factor as mentioned previously.

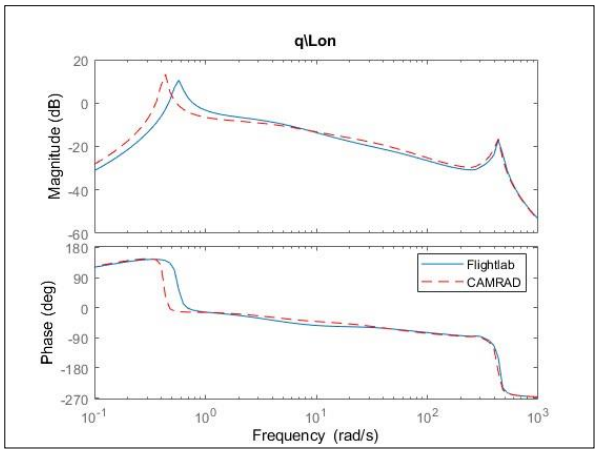

Figure 15. Pitch rate response to longitudinal input

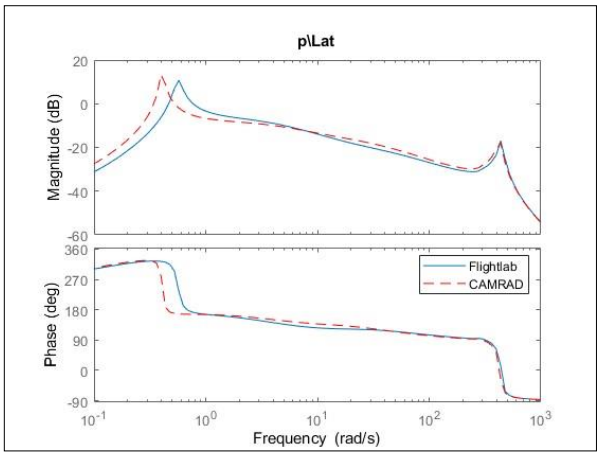

Figure 16. Roll rate response to lateral input

The phugoid mode shown in both pitch and roll rates is present due to the coupling between the attitude and horizontal speed states (Ref. 12). The existence of modes can be understood by looking at the state stability matrix from a simplified model of the longitudinal dynamics.

$$A = \begin{bmatrix} 0 & -g & 0 \\ 0 & 0 & 1 \\ M_u & 0 & 0 \end{bmatrix} \quad (17)$$

Matrix A obtained from (Ref. 12) is restricted to longitudinal dynamics and neglects longitudinal drag X_u and pitch damping M_q. The quantity M_u is the pitch rate sensitivity to a gust hitting the helicopter from the front. As the gust becomes stronger, more nose-up moment is generated. The mode is stabilized by a nose-down moment generated either from the

system M_q or with the help of a control system (with rate feedback). Matrix A has the characteristic equation i.e. $\lambda^3 + M_u g = 0$ with solutions $\lambda_1 = -\sqrt[3]{M_u g}, \lambda_{23} = \frac{1}{2}(1 \pm \sqrt{3}j)\sqrt[3]{M_u g}$ (Ref. 12). The solutions show that the frequency of unstable poles increases with an increase in M_u and g. Even though the phugoid mode is in low frequency, it is still a fundamental factor in designing a control system as it can help impose limitations on the stability margin of the system. The phase shift occurring at different frequencies is due to each tool, i.e., FLIGHTLAB and CAMRAD II predicting different M_u, i.e., 0.2850 for FLIGHTLAB and 0.0080 for CAMRAD II. The difference in M_u is potentially due to the differences in the dynamic inflow wake modeling and wake distortion effect. A coning mode is also present at a higher frequency. This is a coning mode since it exists exactly at the frequency of the rotating flap mode, i.e., 430 rad/s. For control system design purposes, it is important to have no resonant frequencies in mid-range frequencies of 0.1 to 100 rad/s to avoid overworking the actuators. Both longitudinal and lateral rates can be controlled with a control system as there are no resonant frequencies in mid-range frequencies.

Flight Dynamic Analysis in Mars's Atmosphere

Unlike trimming the model in Earth's atmosphere, artificial flap damping is introduced in the system to obtain an equilibrium point when in Mars's atmospheric conditions. Specifically, a $0.85\ \mathrm{kg\,m^2/s}$ flap hinge damping coefficient is introduced. An equilibrium point is computed with this added damping, but the nonlinear dynamics of the hexacopter on Mars are linearized without it. In other words, the flap hinge coefficient of all six rotors is set to zero before extracting linearized models. The extracted models are also validated against linearized models from CAMRAD II.

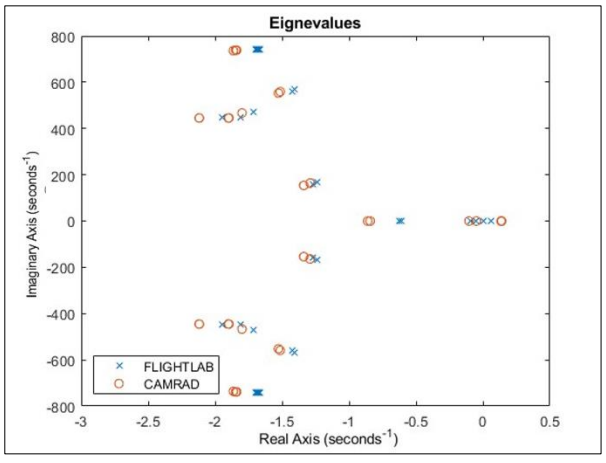

Figure 17. Eigenvalues of Hexacopter in Mars's atmosphere

Figure 17 compares the eigenvalues of the hexacopter in Mars's flight conditions. As seen in the figure, the eigenvalues obtained from FLIGHTLAB match very closely with the eigenvalues from CAMRAD II. Both models consist of higher frequency rotor modes present between the frequency range of 450 to 742 rad/s, and lower frequency airframe modes present between the frequency range of 0.1 to 10 rad/s. As with Earth's atmosphere, inflow modes exist in both low and high-frequency ranges, i.e. 0 to 200 rad/s and 400 to 600 rad/s. The modes presented here are much less damped due to Mars's density being lower than Earth's. Like the hexacopter in Earth's atmosphere, the hexacopter in Mars's atmosphere is also not stable as a set of poles exists in the right-side plane (Figure 18)

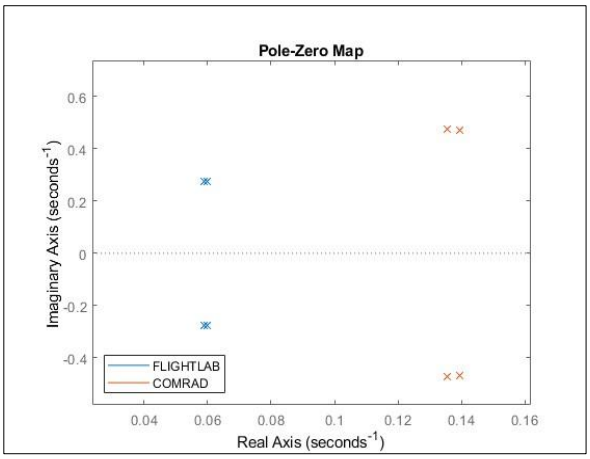

Figure 18. Pole zero map of the hexacopter in Mars's atmosphere

Frequency responses in Mars's atmosphere from FLIGHTLAB are also compared against CAMRAD II. Figure 19 shows the heave response of the hexacopter to collective input. Both responses match very closely with each other, thus validating the heave response. A coning mode is generated in the high-frequency range of the response. The mode is identified as the coning mode as it is generated at the rotating flapping frequency of 448 rad/s. The phase shift in the heave response is very sudden. Specifically, the phase shifts to near zero suddenly due to Mars's atmosphere being low in density making the vehicle lightly damped.

Figure 20 shows a close match between CAMRAD II and FLIGHTLAB's yaw rate response to yaw (pedal) input in Mars's atmosphere. A coning mode is also present in the yaw rate at the rotating natural frequency. A similar characteristic as the heave response is seen with the phase shift to near zero.

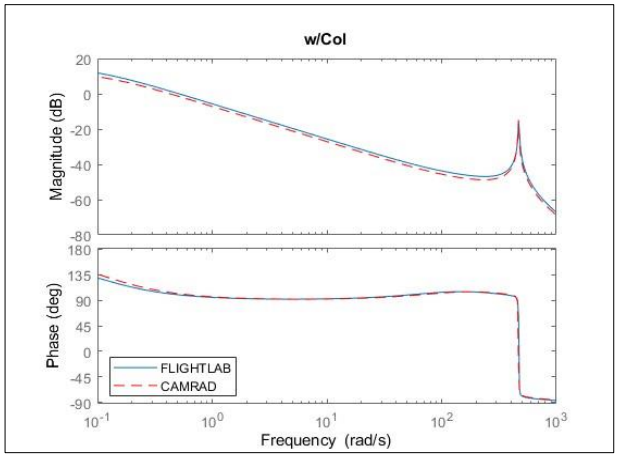

Figure 19. Heave response to collective input in Mars's atmosphere

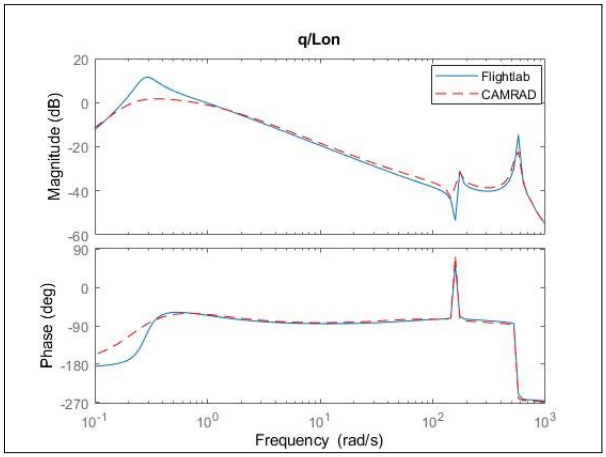

Figure 21. Pitch rate response to longitudinal input in Mars's atmosphere

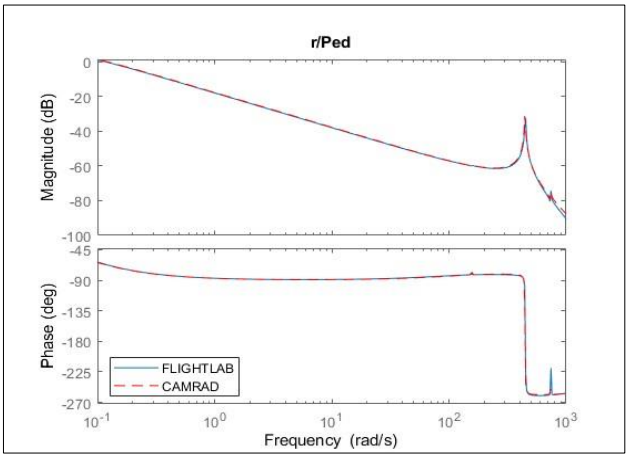

Figure 20. Yaw rate response to pedal input in Mars's atmosphere

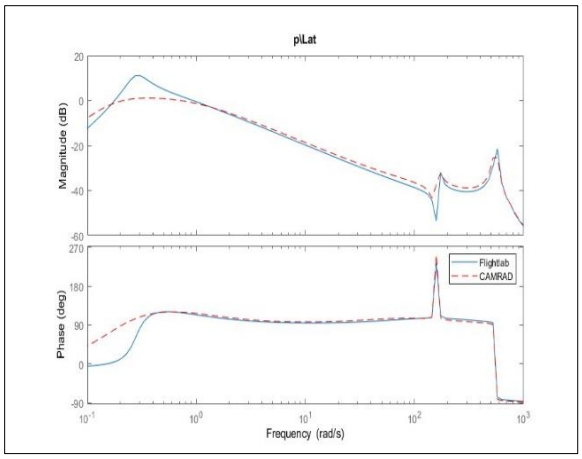

Figure 22.Roll rate response to lateral input in Mars's atmosphere

Figure 21 and Figure 22 show the pitch rate and roll rate response of the hexacopter in Mars's atmosphere respectively. The responses from CAMRAD II and FLIGHTLAB do match closely besides the difference in frequency and damping of phugoid mode, as described previously. The phugoid mode in both CAMRAD II and FLIGHTLAB responses is verified by the existence of unstable poles in the right half plane (Figure 18). The regressive and advancing modes are generated at $\nu_{flap} - 1/rev$ and $\nu_{flap} + 1/rev$ respectively. For the hexacopter operating in Mars's condition with a $\nu_{flap} = 1.54/rev$, the regressive and advancing modes exist at approximately 157 rad/s and approximately 740 rad/s respectively. The coning mode also exists at the rotational flapping frequency of 448 rad/s.

Differences In the Flight Dynamics Between Earth and Mars Environments

Here, the inner loop dynamic characteristic of the hexacopter in both Earth and Mars atmospheres are compared. Figure 23 shows the eigenvalues obtained from FLIGHTLAB's linear model in the Earth and Mars environments. As seen in Figure 23, the rotor (flapping) modes and inflow modes in Earth's atmosphere are more damped than the ones in Mars's environment. This is due to rotors operating at different speeds in each atmosphere which causes all modes on earth to occur at a much lower frequency than they do in Mars's atmosphere.

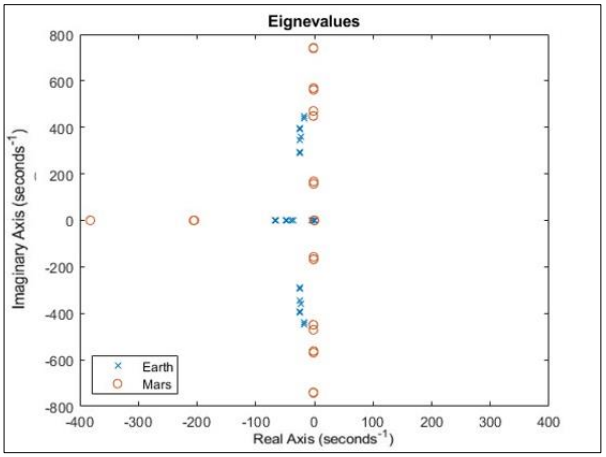

Figure 23. Eigenvalue comparison between Earth and Mars atmospheres

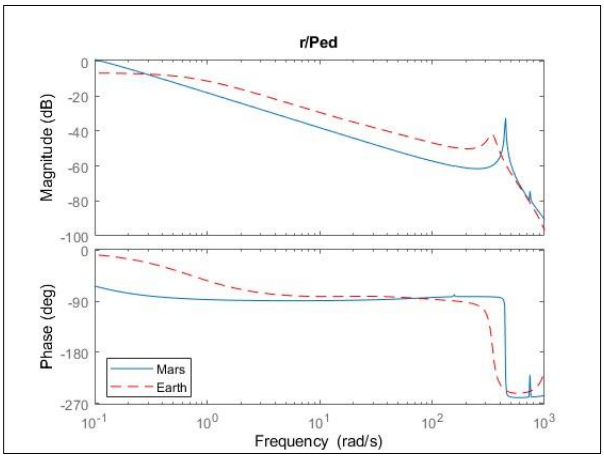

Figure 25. Yaw rate response compared between Earth and Mars atmospheres

Figure 24 and Figure 25 shows the heave and yaw rate response of hexacopter in Mars and Earth atmospheres. Both responses in Mars's atmosphere are damped compared to responses in the Earth's atmosphere. The damped response on Mars is shown by the steep change in the phase angle around the frequency of 450 rad/s (Figure 24 and Figure 25).

The system response at Mars is not as sensitive to the input at the frequency range from 1 rad/s to 400 rad/s. As the system transitions into the mid-range frequencies, the model on Earth is more responsive as there is a lower change in magnitude. At the higher frequency, the Mars model predicts higher magnitude flapping modes due to Mars's density being low. The flapping modes in Mars's atmosphere are higher in magnitude by 10 dB. The differences are further explained in the discussion section below.

A similar dynamic behavior difference is also noticed in both pitch and roll rate responses. The system is not as responsive to Mars's atmospheric conditions as it is in Earth's atmosphere. At 0.1 rad/s, the Mars model reacts more like the model in Earth's atmosphere. The Mars model becomes less responsive past 10 rad/s. Moreover, higher magnitude rotor modes exist in the high-frequency domain. The modes are very less damped than they are in the Earth's atmosphere. Thus, the modes are high in magnitude on Mars than on Earth. The slightly damped modes are confirmed by a not so gradual shift in phase for Mars model, whereas the model operating in Earth's atmosphere is damped as the phase shift is very gradual. The phugoid mode in Mars's gravity has a reduced frequency compared to Earth, as frequency decreases with the decrease in gravity.

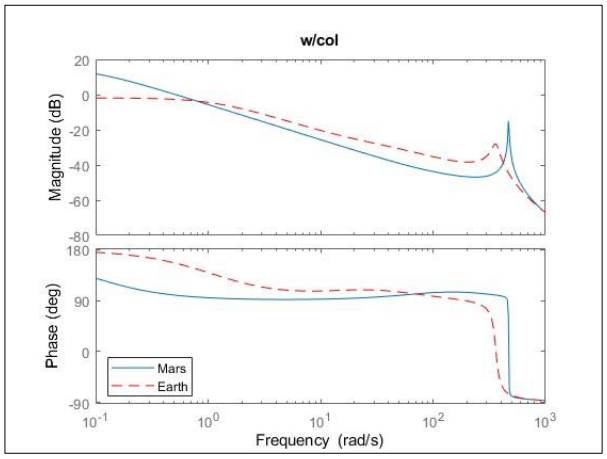

Figure 24. Heave response of the hexacopter in both Earth and Mars atmospheres

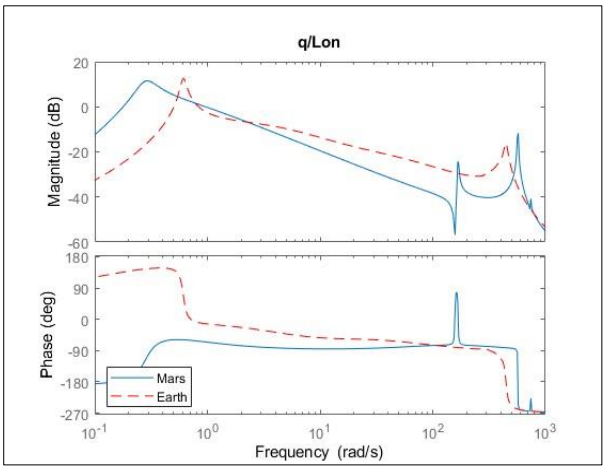

Figure 26. Pitch rate comparison between Earth and Mars atmospheres

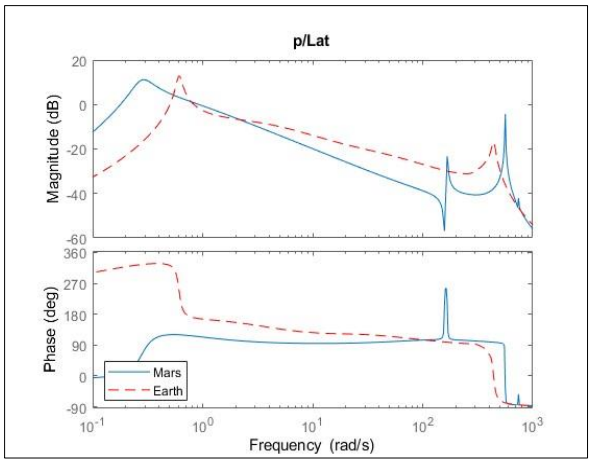

Figure 27. Roll rate response comparison between Earth and Mars atmospheres

DISCUSSION

To better understand the feasibility of designing a dynamically matched surrogate helicopter, a flight dynamics comparison of a closed-loop system between the two environments is needed. Based on the analysis conducted above, it is determined that frequency Bode plots are not sufficient to check if both systems are dynamically similar due to the model being unstable with a non-minimum phase in Mars's atmospheric conditions.

The linear model obtained from FLIGHTLAB predicts the pitch response of the system in Earth's atmosphere being stabilizable. Furthermore, the hexacopter in Earth's atmosphere is also a minimum phase system. Thus, one can predict the stability of the system in Earth's atmosphere by considering the gain and phase margin. The open loop predicts both gain and phase margin of 79 dB and 79 degrees respectively. In the case of a hexacopter operating in Mars's atmospheric conditions, FLIGHTLAB predicts the model to be unstable with a non-minimum phase, thus making the frequency Bode plots not very informative. To determine if the system can be stabilized, Nyquist stability criteria is applied. The Nyquist criteria is based on the number and direction of encirclements of the critical point. The encirclements can be determined interchangeably either from a Nyquist diagram or a Nichols chart. The Nichols chart retains a closer connection to the Bode plot quantities and gain and phase margins can easily be determined from it. Figure 28 shows the pitch response to longitudinal input for the hexacopter operating in both Earth and Mars atmospheres. Here the Nichols chart is used to understand the closed-loop stability of the hexacopter in Mars's atmosphere.

A MIMO system is modeled, therefore, there exist four unstable eigenvalues. Assuming both pitch and roll can be stabilized independently, only two eigenvalues dominate per both pitch and roll response (np=2). Therefore, there are two unstable poles for both pitch and roll responses. As seen in Figure 28, the Mars curve makes two crossovers above the critical point: one above the critical point and one above the critical frequency (phase=180). The two crossovers (N=-2) are equivalent to two counterclockwise encirclements of the critical point in the Nyquist plot. Furthermore, the Nyquist criteria also states that the number of zeros of the characteristic function Q(s)=1+L(s) in the right-hand plane is: Nz=N+np=-2+2=0. Since the pitch response of the hexacopter on Mars has no zeros, the system is stable as zeros of function Q(s) equals the number of poles of T(s) in the right-hand plane. Equation 18 states the transfer function of a closed loop system showing numbers of zeros of Q(s) equals poles of T(s).

$$T(s) = \frac{L(s)}{1+Q(s)} = \frac{L(s)}{Q(s)} \tag{19}$$

Even though the system is stable, the response will still be oscillatory as the phase margin intersects the desirable stability margin block (Figure 28). The Nichols plot gives a phase margin of ~20.5 dB which is less than the desired phase margin of 45 degrees for the system to not be oscillatory.

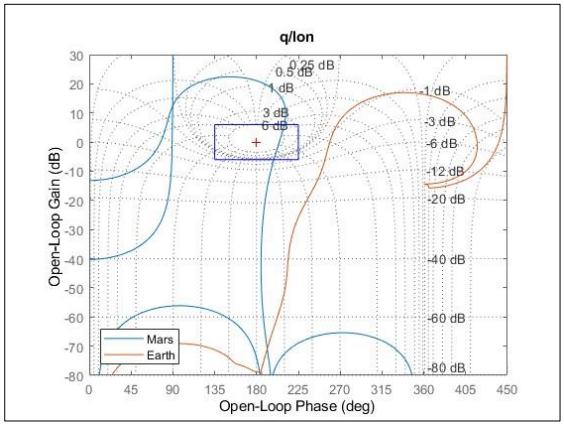

Figure 28. Nichols chart (q/Lon)

In addition to the pitch response of the system in both Earth and Mars atmospheres, the roll response of the vehicle is also analyzed. The roll response on Earth is unstable with a non-minimum phase. Therefore, Nyquist stability criteria must be applied to understand the roll stability of the vehicle. The roll response cannot be stabilized as it gives two clockwise encirclements, thus adding two zeros in the right-hand plane. The phase of roll response can be converted into a minimum phase by inverting the sign of input. Once the input is inverted, mirroring the roll response on Earth (Figure 29) about 180 degrees gives one crossover above the critical point and one above the critical frequency. Then the roll response of the hexacopter on Earth can be stabilized as only two eigenvalues exist that dominate the roll response. The two counterclockwise encirclements of the critical point result in no zeros of the characteristic function Q(s), thus the closed loop transfer function has a zero number of poles in the right-hand plane.

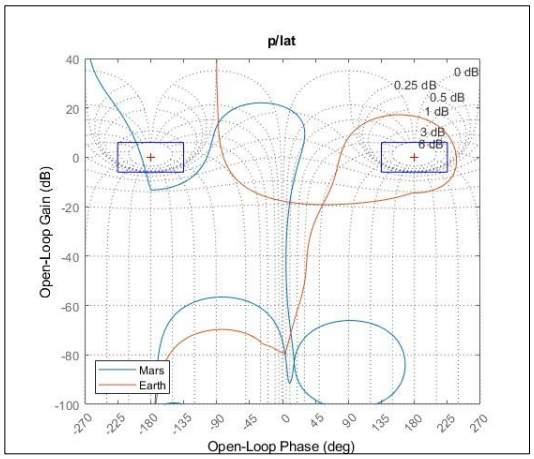

Figure 29. Nichols chart (p/lat)

The flight behavior of the designed hexacopter differs significantly in both the Earth and Mars environments. Specifically, it is easier to stabilize the pitch response of the vehicle on Earth than on Mars due to high gain and phase stability margins on Earth. The closed-loop pitch response on Mars is oscillatory with very small phase margin allowability. In addition, the roll response of the hexacopter is stabilizable on Earth but not so on Mars. Based on the above analysis, the method of proportional gain feedback cannot be applied alone to stabilize both responses on both Earth and Mars environments as that would only decrease stability margins for both pitch and roll response of the hexacopter.

CONCLUSIONS

A comparison of the flight behavior of a hexacopter in both Earth and Mars atmospheres showed different flight characteristics. Specifically, as predicted by FLIGHTLAB the flight responses on Earth differ significantly from the responses on Mars. Below are some of the key findings from the conducted study.

- The rotor flapping modes in Earth's atmosphere are significantly more damped than the responses in the Mars atmosphere.
- The open loop response of the system is unstable in both the Earth and Mars atmospheres. The closed loop response of the hexacopter can be stabilized in Earth's atmosphere and cannot be stabilized in Mars' atmosphere due to having very small phase margin allowability.
- Due to the difference in dynamics of the hexacopter in both atmospheres, it is difficult to determine the control gains required to create a surrogate helicopter.
- A dynamically matched hexacopter that can operate in both atmospheres cannot be designed as the responses in both Earth and Mars atmospheres are not identical to a given input. The technique of proportional feedback is not sufficient to match the dynamic response of both models operating under different environments.

Overall, given the flight dynamics differences mentioned above, it is difficult to design a dynamically matched surrogate hexacopter. Thus, further analysis such as designing an advanced control system that can produce identical responses in both atmospheres with a given input needs to be designed. The advanced control system design can help infer control gains that produce identical responses in both atmospheres. After identical responses are obtained in a hover flight condition, a forward flight configuration can be explored.

Author contact:
Raghuvir Singh raghuvir.singh@nasa.gov

REFERENCES

1. Mars Exploration Program and the Jet Propulsion Laboratory for NASA's Science Mission Directorate, "NASA Science Mars Exploration Program," Jet Propulsion Laboratory , [Online]. Available: https://mars.nasa.gov/#red_planet/5. [Accessed 12 06 2022].

2. "MARS InSight Mission," NASA, [Online]. Available: https://mars.nasa.gov/insight/mission/science/results/. [Accessed 13 06 2022].

3. Grip, H. F., Johnson, W., Malpica, C., Scharf ,D. P., Mandic, M., Young, L., Allan, B., Mettler, B. and Martin, M. S., "Flight Dynamics of Mars Helicopter," 43rd European Rotorcraft Forum, Milan, Italy, 2017.

4. Williams, D., "Mars Fact sheet," NASA Space Science Data Coorinated Archive, 2019. [Online]. Available: https://nssdc.gsfc.nasa.gov/planetary/factsheet/marsfact.html. [Accessed 08 06 2022].

5. "Extreme Planet Takes its Toll," Mars Exploration Rover Mission:Spotlight , 12 June 2007. [Online]. Available: https://mars.nasa.gov/mer/spotlight/20070612.html. [Accessed 13 June 2022].

6. Savu, G. and Trifu, O., "Photovltaic Rotorcraft For Mars Missions," Joint Conference and Exhibit, San Diego, 1995.

7. Kroo, I. and Kunz, P., "Development of the Mesicopter: A Miniature Autonomous Rotorcraft," In Proc. American Helicopter Society Vertical Lift Aircraft Design Conf., San Francisco, 2000.

8. Young, L. A., Chen, R. T. and Aiken, E. W., "Design Opportunites and Challenges in the Development of Vertical Lift Planetary Aerial Vehicles," American Helicopter Scoeity International Vertical Lift Airacraft Design Specialist's Meeting, San Francisco, 2000.

9. Datta, A., Roget, B., Griffiths, D., Pugliese, G., Sitaraman, J., Bao, J., Liu, L. and Gamard, O.,"Design of a Martian Autonomous Rotary-Wing Vehicle," *Journal of Aircraft* , vol. 40, 2003.

10. Lacerda, M., Park, D., Patel, S. and Schrage, D., "A Preliminary systems Engineering Study on a Concept for Mars Exploration with an Unmanned Autonomous Vehicle and Ground Rover," in American Helicopter Society 74th Annual Forum, Phoenix, 2018.

11. Fujita, K., Karaca, H., and Nagai, H. "Parametric Study of Mars Helicopter for Pit Crater Exploration." AIAA Paper No. 2020-1734, January 2020.

12. Grip, H. F., Scharf, D. P., Malpica, C., Johnson, W., Mandic, M., Singh, G. and Young, L., "Guidance and Control for a Mars Helicopter," in *2018 AIAA* Guidance, Navigation, and Control Conference , Kissimmee, Florida , 2018.

13. Johnson, W., Maser, S. W., Young, L., Malpica, C., Koning, W. J., Kuang, W., Fehler, M., Tuano, A., Chan, A., Datta, A., Chi, C., Lumba, R., Escobar, Balaram, D., J., Tzanetos, T. and Grip, H. F., "Mars Science Helicopter Conceptual Design," NASA/TM-2020–220485, 2020.

14. "Component Reference Manual". Advanced Rotorcraft Technology, Inc, Sunnyvale, California.

15. Johnson, W. "CAMRAD II, Comprehensive Analytical Model of Rotorcraft Aerodynamics and Dynamics." Johnson Aeronautics, Palo Alto, California, 1992-1997.

16. Johnson, W., "NDARC. NASA Design and Analysis of Rotorcraft," in NASA TP 2015-218751, 2015.

17. Johnson, W., Rotorcraft Aeromechanics, Cambridge University Press, 2013